TO APPEAR IN APJ VOL. 763 (2013)
Preprint typeset using LaTeX style emulateapj v. 5/2/11

GLOBAL AND LOCAL CUTOFF FREQUENCIES FOR TRANSVERSE WAVES PROPAGATING ALONG SOLAR MAGNETIC FLUX TUBES

S. ROUTH[1], Z. E. MUSIELAK[2,3], AND R. HAMMER[3]
[1]Department of Physics, R.V. College of Engineering, Bangalore, India
[2]Department of Physics, University of Texas at Arlington, Arlington, TX 76019, USA and
[3]Kiepenheuer-Institut für Sonnenphysik, Schöneckstr. 6, Freiburg, D–79104 Germany
(Received 2012 July 29; Accepted 2012 December 4)
to appear in ApJ Vol. 763 (2013)

ABSTRACT

It is a well-established result that the propagation of linear transverse waves along a thin but isothermal magnetic flux tube is affected by the existence of the global cutoff frequency, which separates the propagating and non-propagating waves. In this paper, the wave propagation along a thin and non-isothermal flux tube is considered and a local cutoff frequency is derived. The effects of different temperature profiles on this local cutoff frequency are studied by considering different power-law temperature distributions as well as the semi-empirical VAL C model of the solar atmosphere. The obtained results show that the conditions for wave propagation strongly depend on the temperature gradients. Moreover, the local cutoff frequency calculated for the VAL C model gives constraints on the range of wave frequencies that are propagating in different parts of the solar atmosphere. These theoretically predicted constraints are compared to observational data and are used to discuss the role played by transverse tube waves in the atmospheric heating and dynamics, and in the excitation of solar atmospheric oscillations.

Subject headings: magnetohydrodynamics (MHD) – Sun: atmosphere – waves

1. INTRODUCTION

Magnetic flux tubes existing in the photosphere and lower chromosphere of the Sun are considered to be narrow bundles of strong magnetic field lines that rapidly expand with height in the solar atmosphere (e.g., Solanki 1993). The fundamental modes of linear oscillations of these flux tubes are typically identified with longitudinal, transverse and torsional tube waves (e.g., Defouw 1976; Roberts & Webb 1978; Roberts 1979, 1981; Spruit 1981, 1982; Priest 1982; Hollweg 1985; Roberts 1991; Roberts & Ulmschneider 1997), with the two latter waves being Alfvén-like waves.

Observational evidence for the existence of Alfvén-like waves in different regions of the solar atmosphere was given by high-resolution observations performed by the Solar Optical Telescope (SOT) and the X-Ray Telescope (XRT) onboard the Hinode Solar Observatory. According to De Pontieu et al. (2007) and Cirtain et al. (2007), signatures of Alfvén waves were observed by the SOT and XRT instruments, respectively. Moreover, Alfvén waves were also reported by Tomczyk et al. (2007), who used the Coronal Multi-Channel Polarimeter of the National Solar Observatory. Interpretations of these observations were given by Van Doorsselaere et al. (2008) and Antolin et al. (2009), who concluded that the reported observational results describe kink waves. As of today, the most convincing observational evidence for the existence of Alfvén waves in the quiescent solar atmosphere was given by McIntosh et al. (2011), who reported indirect evidence for such waves found in observations by Solar Dynamic Observatory (SDO).

Moreover, Fujimura & Tsuneta (2009) used SOT observations to study fluctuations in pores and intergranular magnetic structures, and concluded that such fluctuations could be explained by the existence of longitudinal (sausage) and transverse (kink) waves propagating along magnetic flux tubes embedded in the solar photosphere. They found oscillation periods of 3-6 min for the pores and 4-9 min for the intergranular magnetic elements. More recently, Okamoto and De Pontieu (2011) used data from SOT and presented observational evidence for the existence of high-frequency transverse waves propagating along spiclues in the solar atmosphere. Similar high-frequency tranverse waves were reported by Yurchyshyn et al. (2012), who observed type II spicules using the New Solar Telescope.

There is also observational evidence for the existence of torsional Alfvén waves in the solar atmosphere as reported by Jess et al. (2009), who interpreted data obtained with high spatial resolution by the Swedish Solar Telescope (SST). Alfvén-like motions were also observed by Bonet et al. (2008), who found vortex motions of G band bright points around downflow zones in the solar photosphere, and by Wedemeyer-Böhm & Rouppe van der Voort (2009), who used data from the SST to demonstrate that more disorganized relative motions of photospheric bright points can also induce swirl-like motions in the solar chromosphere. More recently, observational evidence for Alfvén-like waves was found by Bonet et al. (2010), who used the ballon-borne Sunrise Telescope, and by De Pontieu et al. (2012), who used the SST to find torsional motions in spicules. Moreover, magnetic swirls in the solar atmosphere were reported by Wedemeyer-Böhm et al. (2012).

Among the above described observational results, the observations perfomed by Fujimura & Tsuneta (2009), Okamoto and De Pontieu (2011), and Yurchyshyn et al. (2012) are the most relevant because the authors directly refer to transverse tube waves, which are the main topic of this paper. Our goal here is to determine the propagation conditions for these waves by calculating the so-called cutoff frequencies. In general, there are global cutoff frequencies, which are the same along the entire length of the tube, and local cutoff frequen-

swati.routh@lcd.co.edu
zmusielak@uta.edu
hammer@kis.uni-freiburg.de

cies that are height dependent. If, under certain simplifying approximations, the cutoff frequency is constant along the entire length of the tube, it is called a global cutoff. Otherwise, if it is height dependent, it is a local cutoff. In Section 6, we compare these cutoff frequencies to the observational results.

The global cutoff frequency represents the natural frequency of linear oscillations of the magnetic flux tubes, and its value restricts the wave propagation to only those frequencies that are higher than this cutoff. For isothermal and thin flux tubes, the global cutoff frequencies for longitudinal and transverse tube waves were first determined by Defouw (1976) and Spruit (1981), respectively. These global cutoff frequencies are ratios of the characteristic wave speeds to the pressure (density) scale height. Since the scale height and the wave speeds are constant along isothermal and exponentially expanding magnetic flux tubes, the resulting cutoffs are the same along the entire length of the tubes. The fact that there is no global cutoff frequency for torsional waves propagating along isothermal and thin magnetic flux tubes was demonstrated by Musielak, Routh & Hammer (2007).

A method to derive the global cutoff frequency for longitudinal tube waves was introduced by Rae & Roberts (1982) and Musielak et al. (1987, 1995), who demonstrated that the wave equation for these waves can be transformed into its standard form (also referred to as the Klein-Gordon equation), which directly displays the global cutoff frequency. A similar method was used by Musielak & Ulmschneider (2001, 2003) to determine the global cutoff frequency for transverse tube waves. These global cutoff frequencies are important in studies of atmospheric oscillations (e.g., Roberts 1991; Hasan & Kalkofen 1999; Hasan 2003; Musielak & Ulmschneider 2003; Hasan 2008) and chromospheric and coronal heating (e.g., Narain & Ulmschneider 1996; Ulmschneider & Musielak 2003).

The existence of global cutoff frequencies is restricted to thin and isothermal magnetic flux tubes. However, in more general cases when the flux tubes are either wide and isothermal, or thin and non-isothermal, or wide and non-isothermal, the resulting cutoff frequencies depend on atmospheric height, which means that they are local quantities (e.g., Routh, Musielak & Hammer 2007). A method to determine such local cutoff frequencies was developed by Musielak, Musielak & Mobashi (2006). This method requires that wave equations are cast in their standard forms (i.e.,without terms with the first-order derivatives) and that the oscillation theorem (e.g., Kahn 1990) is used to obtain the cutoff frequencies.

The form of the oscillation theorem used in this paper is that given by Kahn (1990). Different forms of this theorem were considered by mathematicians depending on specific differential equations and the applied boundary conditions. The basic idea was originally introduced by Sturm (1836), who considered a second-order ordinary differential equation written in its standard form and established a comparison criterion, which allowed him to determine whether solutions to the equation were oscillatory or not, without formally solving the equation. Another comparison criterion was developed by Kneser (1893) and later generalized by Fite (1918), Hille (1948), Wintner (1949, 1957), and many others. The most important generalization of Kneser's criterion was done by Leighton (1950, 1962). In more recent work, some oscillation theorems were established for linear (e.g., Li & Yeh 1995, 1996) and nonlinear (e.g., Li 1998; Lee et al. 2005; Tyagi 2009) second-order differential equations.

The oscillation theorem presented by Kahn (1990), which is used in this paper, is equivalent to Kneser's criterion, which is also known as Kneser's theorem (e.g., Bohner & Ünal 2005). First applications of this theorem to solar physics problems were done by Musielak & Moore (1995), who considered the propagation of linear Alfvén waves in an isothermal solar atmosphere. Then, Schmitz & Fleck (1998) used the theorem to establish criteria for acoustic wave propagation in the solar atmosphere. More recently the theorem was used by Schmitz & Fleck (2003), Musielak et al. (2006, 2007), Routh et al. (2007, 2010), and Hammer et al. (2010).

In this paper, we use this method to derive the cutoff frequency for transverse waves propagating along a thin and non-isothermal magnetic flux tube embedded in the solar atmosphere. The effects of temperature gradients on the cutoff frequency are studied for several power-law temperature models as well as for the reference mean solar atmosphere model C given by Vernazza, Avrett & Loeser (1981). The height dependence of the cutoff frequency in these models is calculated, and it is shown that the value of this cutoff at a given atmospheric height determines the frequency that transverse tube waves must exceed in order to be propagating at this height. The results are compared to those previously obtained for a thin and isothermal magnetic flux tube. We also briefly discuss implications of our results for the energy and momentum balance of the solar atmosphere.

Our paper is organized as follows: the governing equations and derivation of our wave equations are given in Section 2; the global cutoff frequency for linear transverse waves propagating along a thin and isothermal magnetic flux tube is obtained in Section 3; the local cutoff frequency for the wave propagation along a thin and non-isothermal magnetic flux tube is derived in Section 4; the local cutoff frequencies for different power-law temperature distributions and for the VAL C solar atmosphere model are presented and discussed in Sections 5 and 6, respectively; and conclusions are given in Section 7.

2. WAVE EQUATIONS

We consider a thin and non-isothermal magnetic flux tube that is embedded in the solar atmosphere. The tube axis is assumed to have a circular cross-section and an unperturbed tube axis oriented vertically along the z-axis, so that gravity $\vec{g} = -g\hat{z}$. The tube density, pressure, temperature, and magnetic field are respectively given by $\rho_0 = \rho_0(z)$, $p_0 = p_0(z)$, $T_0 = T_0(z)$, and $B_0 = B_0(z)$. Moreover, the density, pressure and temperature of the external non-magnetic ($B_e = 0$) atmosphere are represented by $\rho_e = \rho_e(z)$, $p_e = p_e(z)$ and $T_e = T_e(z)$, respectively. We assume that the tube is in thermal equilibrium with its surroundings, which means that at each atmospheric height $T_0(z) = T_e(z)$.

In the thin flux tube approximation (e.g., Ferriz-Mas et al. 1989), the horizontal pressure balance for the tube becomes

$$p_0 + \frac{B_0^2}{8\pi} = p_e \ . \tag{1}$$

The equation for transverse linear oscillations of the tube was originally derived by Spruit (1981), who obtained

$$\frac{\partial^2 \xi}{\partial t^2} - c_{\rm k}^2(z)\,\frac{\partial^2 \xi}{\partial z^2} - g\frac{\rho_0 - \rho_e}{\rho_0 + \rho_e}\frac{\partial \xi}{\partial z} = 0 \ , \tag{2}$$

where ξ is the horizontal displacement of the tube, and $c_{\rm k}$ is

the characteristic wave speed given by

$$c_{\rm k}(z) = \frac{B_0}{\sqrt{4\pi(\rho_0+\rho_e)}} \ . \tag{3}$$

The relationship between the displacement ξ and the corresponding magnetic field perturbation b_x was obtained by Stix (1991) and Bogdan et al. (1996), and it can be written as

$$b_x = B_0 \frac{\partial \xi}{\partial z} \ . \tag{4}$$

Defining the velocity perturbation

$$v_x = \frac{\partial \xi}{\partial t} \ , \tag{5}$$

and using

$$g\frac{\rho_0-\rho_e}{\rho_0+\rho_e} = -\frac{c_{\rm k}^2}{2H} \ , \tag{6}$$

where $H = c_{\rm S}^2/\gamma g$ is the pressure scale height, with γ being the ratio of specific heats and $c_{\rm S}$ being the speed of sound given by $c_{\rm S} = \sqrt{\gamma p_0/\rho_0}$, we write Equation (2) in the following form

$$\frac{\partial^2 v_x}{\partial t^2} - c_{\rm k}^2(z)\,\frac{\partial^2 v_x}{\partial z^2} + \frac{c_{\rm k}^2(z)}{2H(z)}\,\frac{\partial v_x}{\partial z} \ = 0 \ . \tag{7}$$

Then we combine Equations (2) and (4), use $dB_0/dz = -B_0/2H$, and obtain

$$\frac{\partial^2 b_x}{\partial t^2} - c_{\rm k}^2(z)\,\frac{\partial^2 b_x}{\partial z^2} - c_{\rm k}^2(z)\left[\frac{2}{c_{\rm k}(z)}\left(\frac{dc_{\rm k}(z)}{dz}\right) + \frac{1}{2H(z)}\right]\frac{\partial b_x}{\partial z} = 0 \ . \tag{8}$$

The derived wave equations describe the propagation of linear transverse waves along a thin and non-isothermal magnetic flux tube. Since the wave equations for v_x and b_x are different, there is a phase difference between the wave variables. Physical consequences of the existence of this phase shift will be explored in the next sections.

3. GLOBAL CUTOFF FREQUENCY

We now consider the special case of a thin and isothermal magnetic flux tube by taking T_0 = const, T_e = const and $T_0 = T_e$, which gives $c_{\rm k}$ = const and H = const. This allows us to write the wave equations (see Equations (7) and (8)) as

$$\frac{\partial^2 v_x}{\partial t^2} - c_{\rm k}^2\,\frac{\partial^2 v_x}{\partial z^2} + \frac{c_{\rm k}^2}{2H}\,\frac{\partial v_x}{\partial z} \ = 0 \tag{9}$$

and

$$\frac{\partial^2 b_x}{\partial t^2} - c_{\rm k}^2\,\frac{\partial^2 b_x}{\partial z^2} - \frac{c_{\rm k}^2}{2H}\,\frac{\partial b_x}{\partial z} \ = 0 \ . \tag{10}$$

Comparison of the above wave equations shows that they are different, which means that the behavior of the wave variables v_x and b_x is different even for a thin and isothermal flux tube.

The wave equation for v_x was originally obtained by Spruit (1981, 1982) and he showed that the propagation of transverse waves along a thin and isothermal magnetic flux tube is affected by a cutoff frequency. A new result presented in this paper is that we also derive the wave equation for b_x, show that it is different than the one obtained for v_x, and demonstrate how to obtain the cutoff frequency for both wave variables.

To obtain the cutoff frequency, we follow Musielak & Ulmschneider (2001) and cast Equations (9) and (10) into their standard (or Klein-Gordon) forms (e.g., Roberts 1981; Rae & Roberts 1982). The required transformations are $v_x(z,t) = v_1(z,t)\rho_0^{-1/4}(z)$ and $b_x(z,t) = b_1(z,t)\rho_0^{1/4}(z)$, and the resulting wave equations can be written as

$$\left[\frac{\partial^2}{\partial t^2} - c_{\rm k}^2\frac{\partial^2}{\partial z^2} + \Omega_{\rm k}^2\right]\ [v_1(z,t), b_1(z,t)] \ = 0 \ , \tag{11}$$

where

$$\Omega_{\rm k} = \frac{c_{\rm k}}{4H} \tag{12}$$

is called here Spruit's cutoff frequency. Since $c_{\rm k}$ = const and H = const in the isothermal case, $\Omega_{\rm k}$ is also constant, which means that it is a global quantity.

With the coefficients of Equation (11) being constant, we can make Fourier transforms in time and space, and derive the global dispersion relation: $(\omega^2 - \Omega_{\rm k}^2) = k^2 c_{\rm k}^2$, where ω is the wave frequency and $k = k_z$ is the wave vector along the tube axis. Based on this dispersion relation, $\Omega_{\rm k}$ is the global cutoff frequency for transverse tube waves. According to the dispersion relation, the waves are propagating when $\omega > \Omega_{\rm k}$ and k is real, and non-propagating when either $\omega = \Omega_{\rm k}$ with $k = 0$ or $\omega < \Omega_{\rm k}$ with k being imaginary; in the latter case, the waves are called evanescent waves.

According to Musielak et al. (2006, 2007) and Petukhov (2006), gradients of restoring forces, which can introduce characteristic scale heights, are responsible for the origin of cutoff frequencies for different waves. Using this argument, Musielak et al. (2006) argued about the origin of the acoustic cutoff frequency and Musielak et al. (2007) showed that the propagation of torsional tube waves is cutoff-free. Moreover, Petukhov (2006) demonstrated that horizontal, non-uniform but potential magnetic fields have no influence on a cutoff frequency for magneto-acoustic waves and, as a result, the cutoff is identical to Lamb's cutoff frequency, $\Omega_{\rm S} = c_{\rm S}/2H$, which was obtained by Lamb (1908, 1975) for acoustic waves propagating in a stratified and isothermal medium.

The results obtained here for transverse tube waves clearly show that the vertical and non-uniform (exponentially diverging) magnetic field of a thin and isothermal flux tube is responsible for the origin of Spruit's cutoff frequency. Actually, the existence of this cutoff is caused by the horizontal pressure balance, which relates the tube magnetic pressure to the gas pressure. Since the latter introduces the pressure scale height H that also determines the rate with which the field diverges with the atmospheric height, the tube magnetic field and its characteristic scale height are the main physical reasons for the existence of Spruit's cutoff frequency.

Finally, we may relate the Spruit cutoff $\Omega_{\rm k}$ to the Lamb cutoff $\Omega_{\rm S}$ by writing

$$\Omega_{\rm k} = \frac{1}{2}\frac{c_{\rm k}}{c_{\rm S}}\Omega_{\rm S} \ , \tag{13}$$

which shows that the ratio of $c_{\rm k}$ to $c_{\rm S}$ determines how much $\Omega_{\rm k}$ differs from $\Omega_{\rm S}$. For the special case $c_{\rm k} = c_{\rm S}$, we have $\Omega_{\rm k} = \Omega_{\rm S}/2$. Hence, $\Omega_{\rm k}$ can be much larger than $\Omega_{\rm S}$ when $c_{\rm k} >> c_{\rm S}$ and much smaller when $c_{\rm k} << c_{\rm S}$.

4. LOCAL CUTOFF FREQUENCY

We now consider a thin but non-isothermal magnetic flux tube whose internal temperature distribution is $T_0 = T_0(z)$, and assume that at each atmospheric height the tube is in thermal equilibrium with its surroundings, which means that $T_0(z) = T_e(z)$. The presence of temperature gradients makes both $c_{\rm k}$

and H to be functions of z, and this leads to wave equations for v_x and b_x that have non-constant coefficients (see Equations (9) and (10)).

Since these wave equations cannot be solved by using Fourier transforms in space, a different method to obtain cutoff frequencies is required. Such a method was originally developed by Musielak et al. (2006) for acoustic waves propagating in non-isothermal media. Routh et al. (2007, 2010) and Hammer et al. (2010) used the method to determine cutoff frequencies for the propagation of torsional waves in thick (isothermal) and thin (non-isothermal) magnetic flux tubes. Here, this method will be used to derive local cutoff frequencies for transverse waves propagating along a thin flux tube with different temperature profiles.

The method is based on the oscillation theorem given by Kahn (1990), which follows the original work of Sturm (1836) and Kneser (1893). Actually, there are numerous oscillation theorems developed by mathematicians for various differential equations and their boundary conditions (e.g., Swanson 1968; Teschl 2011, and references therein). However, most of these theorems cannot be directly applied to Euler's equation (e.g., Wong 1996; Aghajani & Roomi 2012), which is used in this paper. Fortunately, solutions to Euler's equations are well-known (e.g., Murphy 1960), and they form the basis for our method used in this paper.

4.1. *Transformed wave equations*

The method begins with introducing a new variable

$$d\tau = \frac{dz}{c_{\rm k}(z)} \ . \tag{14}$$

The physical meaning of this variable becomes obvious after both sides of the above equation are integrated (see below). Then, $\tau(z)$ is the actual wave travel time between a height at which a wave source is located and a given height z along the axis of the magnetic flux tube.

We express Equations (7) and (8) in terms of the variable τ and obtain the following transformed wave equations

$$\left[\frac{\partial^2}{\partial t^2} - \frac{\partial^2}{\partial \tau^2} + \left(\frac{c'_{\rm k}}{c_{\rm k}} + \frac{c_{\rm k}}{2H}\right)\frac{\partial}{\partial \tau}\right] v_x(\tau,t) \ = 0 \tag{15}$$

and

$$\left[\frac{\partial^2}{\partial t^2} - \frac{\partial^2}{\partial \tau^2} - \left(\frac{c'_{\rm k}}{c_{\rm k}} + \frac{c_{\rm k}}{2H}\right)\frac{\partial}{\partial \tau}\right] b_x(\tau,t) \ = 0 \ , \tag{16}$$

where $c_{\rm k} = c_{\rm k}(\tau)$, $c'_{\rm k} = dc_{\rm k}/d\tau$ and $H = H(\tau)$.

4.2. *Standard wave equations*

To convert the transformed wave equations into their standard forms, we use

$$v_x(\tau,t) = v(\tau,t)\exp\left[+\frac{1}{2}\int^{\tau}\left(\frac{c'_{\rm k}}{c_{\rm k}} + \frac{c_{\rm k}}{2H}\right)d\tilde{\tau}\right] \tag{17}$$

and

$$b_x(\tau,t) = b(\tau,t)\exp\left[-\frac{1}{2}\int^{\tau}\left(\frac{c'_{\rm k}}{c_{\rm k}} + \frac{c_{\rm k}}{2H}\right)d\tilde{\tau}\right] \ , \tag{18}$$

and obtain

$$\left[\frac{\partial^2}{\partial t^2} - \frac{\partial^2}{\partial \tau^2} + \Omega^2_{{\rm cr},v}(\tau)\right] v(\tau,t) = 0 \tag{19}$$

and

$$\left[\frac{\partial^2}{\partial t^2} - \frac{\partial^2}{\partial \tau^2} + \Omega^2_{{\rm cr},b}(\tau)\right] b(\tau,t) = 0 \ , \tag{20}$$

where

$$\Omega^2_{{\rm cr},v}(\tau) = \Omega^2_{\rm k}(\tau) + \frac{3}{4}\left(\frac{c'_{\rm k}}{c_{\rm k}}\right)^2 - \frac{1}{2}\frac{c''_{\rm k}}{c_{\rm k}} + \frac{c_{\rm k}}{4H}\,\frac{H'}{H} \tag{21}$$

and

$$\Omega^2_{{\rm cr},b}(\tau) = \Omega^2_{\rm k}(\tau) - \frac{1}{4}\left(\frac{c'_{\rm k}}{c_{\rm k}}\right)^2 + \frac{1}{2}\frac{c''_{\rm k}}{c_{\rm k}} - \frac{c_{\rm k}}{4H}\,\frac{H'}{H} + \frac{c'_{\rm k}}{2H} \ , \tag{22}$$

with $c''_{\rm k} = d^2c_{\rm k}/d\tau^2$ and $H' = dH/d\tau$. The frequencies $\Omega_{{\rm cr},v}$ and $\Omega_{{\rm cr},b}$ are known as the critical frequencies (Musielak et al. 1992, 2006).

4.3. *Turning-point frequencies*

We make the Fourier transform in time $[v(\tau,t), b(\tau,t)] = [\tilde{v}(\tau), \tilde{b}(\tau)]e^{-i\omega t}$, where ω is the wave frequency, and write Equations (19) and (20) as

$$\left[\frac{d^2}{d\tau^2} + \omega^2 - \Omega^2_{{\rm cr},v}(\tau)\right]\tilde{v}(\tau) = 0 \tag{23}$$

and

$$\left[\frac{d^2}{d\tau^2} + \omega^2 - \Omega^2_{{\rm cr},b}(\tau)\right]\tilde{b}(\tau) = 0 \ . \tag{24}$$

Using the oscillation theorem given by Kahn (1990) and comparing the above equations to Euler's equation (e.g., Murphy 1960), we obtain the following conditions for the wave propagation

$$\omega^2 - \Omega^2_{{\rm cr},v}(\tau) > \frac{1}{4\tau^2} \tag{25}$$

and

$$\omega^2 - \Omega^2_{{\rm cr},b}(\tau) > \frac{1}{4\tau^2} \ . \tag{26}$$

Note that applications of the oscillation theorem to other wave propagation problems relevant to solar physics were previously considered by Musielak & Moore (1995) and Schmitz & Fleck (1998); see also Routh et al. (2010) for more recent results. The idea of using Euler's equation to determine turning-point frequencies was first introduced by Musielak & Moore (1995).

We follow Musielak et al. (2006) and define the turning-point frequencies as

$$\Omega^2_{{\rm tp},v}(\tau) = \Omega^2_{{\rm cr},v}(\tau) + \frac{1}{4\tau^2} \tag{27}$$

and

$$\Omega^2_{{\rm tp},b}(\tau) = \Omega^2_{{\rm cr},b}(\tau) + \frac{1}{4\tau^2} \ , \tag{28}$$

where τ is the actual wave propagation time (see Routh et al. 2010) and is given by

$$\tau(z) = \int^{z}\frac{d\tilde{z}}{c_{\rm k}(\tilde{z})} + \tau_C \ , \tag{29}$$

with τ_C being an integration constant to be evaluated when flux tube models are specified (see Sections 6 and 7).

It is important to point out that the turning-point frequencies were obtained by making the derived wave equations (see

Equations (23) and (24)) equivalent to Euler's equation, so that the well-known solutions of the latter can be directly applied to these wave equations.

4.4. *Converting τ into z*

Having obtained the turning-point frequencies (see Equations (27) and (28)), we now express them in terms of the z variable, which requires using Equation (29) to convert τ to z.

We begin with the critical frequencies $\Omega_{\mathrm{cr},v}(\tau)$ and $\Omega_{\mathrm{cr},b}(\tau)$ given by Equations (21) and (22). Using the following expressions

$$\frac{1}{c_\mathrm{k}}\frac{dc_\mathrm{k}}{d\tau} = \frac{dc_\mathrm{k}}{dz}\ , \tag{30}$$

$$\frac{1}{c_\mathrm{k}}\frac{d^2c_\mathrm{k}}{d\tau^2} = c_\mathrm{k}\frac{d^2c_\mathrm{k}}{dz^2} + \left(\frac{dc_\mathrm{k}}{dz}\right)^2\ , \tag{31}$$

and

$$\frac{1}{c_\mathrm{k}}\frac{dH}{d\tau} = \frac{dH}{dz}\ , \tag{32}$$

we obtain

$$\Omega^2_{\mathrm{cr},v}(z) = \Omega^2_\mathrm{k}(z)\left[1+4\left(\frac{dH}{dz}\right)\right] - \frac{1}{2}c_\mathrm{k}\frac{d^2c_\mathrm{k}}{dz^2} + \frac{1}{4}\left(\frac{dc_\mathrm{k}}{dz}\right)^2\ , \tag{33}$$

and

$$\Omega^2_{\mathrm{cr},b}(z) = \Omega^2_\mathrm{k}(z)\left[1-4\left(\frac{dH}{dz}\right)\right] + \frac{c_\mathrm{k}}{2H}\frac{dc_\mathrm{k}}{dz} + \frac{1}{2}c_\mathrm{k}\frac{d^2c_\mathrm{k}}{dz^2} + \frac{1}{4}\left(\frac{dc_\mathrm{k}}{dz}\right)^2\ , \tag{34}$$

We now use Equation (29) to express the conditions for wave propagation and the turning-point frequencies as functions of z, and obtain

$$\left[\omega^2 - \Omega^2_{\mathrm{cr},v}(z)\right] > \frac{1}{4}\left[\int^z \frac{d\tilde{z}}{c_\mathrm{k}(\tilde{z})} + \tau_C\right]^{-2} \tag{35}$$

and

$$\left[\omega^2 - \Omega^2_{\mathrm{cr},b}(z)\right] > \frac{1}{4}\left[\int^z \frac{d\tilde{z}}{c_\mathrm{k}(\tilde{z})} + \tau_C\right]^{-2}\ . \tag{36}$$

The turning-point frequencies are

$$\Omega^2_{\mathrm{tp},v}(z) = \Omega^2_{\mathrm{cr},v}(z) + \frac{1}{4}\left[\int^z \frac{d\tilde{z}}{c_\mathrm{k}(\tilde{z})} + \tau_C\right]^{-2} \tag{37}$$

and

$$\Omega^2_{\mathrm{tp},b}(z) = \Omega^2_{\mathrm{cr},b}(z) + \frac{1}{4}\left[\int^z \frac{d\tilde{z}}{c_\mathrm{k}(\tilde{z})} + \tau_C\right]^{-2}\ . \tag{38}$$

We shall use the turning-point frequencies given above to determine the cutoff frequency for transverse tube waves.

4.5. *Cutoff frequency*

We follow Musielak et al. (2006) and take the larger of the two turning-point frequencies to be the cutoff frequency Ω_cut,

$$\Omega_\mathrm{cut}(z) = \max[\Omega_{\mathrm{tp},v}(z), \Omega_{\mathrm{tp},b}(z)]\ . \tag{39}$$

Our selection of Ω_cut is physically justified by the fact that in order to have propagating transverse tube waves, the wave frequency ω must always be higher than any turning-point frequency. In other words, the choice guarantees that propagating wave solutions are obtained for both wave variables, and that the cutoff frequency does separate the propagating and non-propagating wave solutions (see also Hammer et al. 2010). Hence, the condition for propagating waves is $\omega > \Omega_\mathrm{cut}$. Based on our definition of the turning-point frequencies, the condition for non-propagating (evanescent) waves is $\omega \leq \Omega_\mathrm{cut}$.

The above results show that the cutoff frequency can only be determined when a flux tube model is specified, so that the turning-point frequencies can be obtained (see Sections 5 and 6). In addition, one must keep in mind that the conditions given by Equation (39) must be checked at each height because in some regions along the tube $\Omega_{\mathrm{tp},v}$ could be larger than $\Omega_{\mathrm{tp},b}$, and the opposite could be true in other regions (see Section 6).

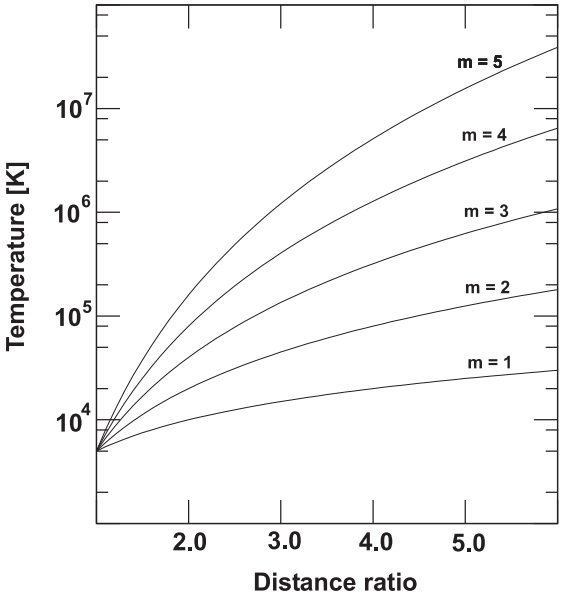

Figure 1. Temperature is plotted versus the distance ratio z/z_0 for the power-law temperature models with m ranging from 1 to 5.

5. MODELS WITH POWER-LAW TEMPERATURE DISTRIBUTIONS

Let us consider the following temperature distribution inside the tube

$$T_0(z) = T_{00}\xi^m\ , \tag{40}$$

where $\xi = z/z_0$ is the distance ratio, with z_0 being a fixed height in the model, T_{00} is the temperature at z_0, and m can be any real number. Note that in all power-law models discussed below a wave source is assumed to be located at $\xi = 1$, which means that in all calculations $\xi \geq 1$. In addition, for all models we take $z_0 = 10$ km, $T_{00} = 5000$ K, $c_{\mathrm{k}0} = 10$ km/s, and for gravity we take its solar value. The resulting temperature distributions for m being a positive integer that ranges from 1 to 5 are presented in Figure 1.

5.1. *Case of m = 1*

To describe the process of deriving a local cutoff frequency, we begin with the simplest case of $m = 1$, which corresponds to the temperature varying linearly with ξ. We calculate ρ_0,

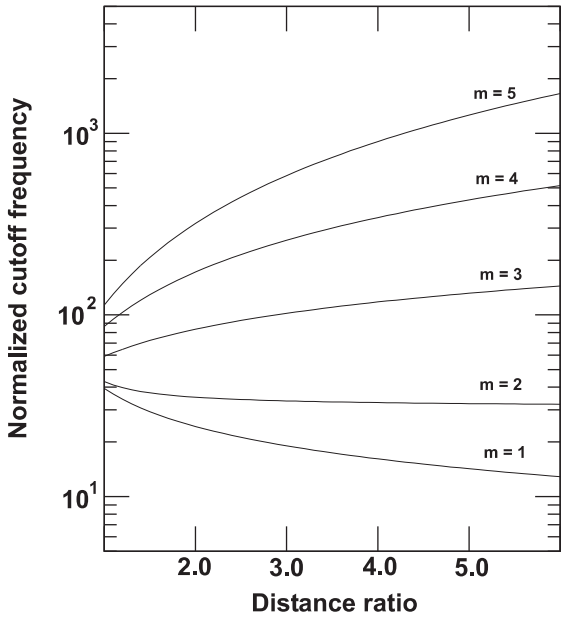

Figure 2. The normalized cutoff frequency $\Omega_{\rm cut}/\Omega_{\rm k0}$ is plotted versus the distance ratio z/z_0 for the power-law temperature models with m ranging from 1 to 5.

p_0, B_0 and $c_{\rm k}$ as functions of ξ, and use Equation (29) to obtain

$$\tau(\xi) = 2\frac{z_0}{c_{\rm k0}}\xi^{1/2} + \tau_C \ , \tag{41}$$

where $c_{\rm k0}$ is the value of $c_{\rm k}$ at z_0 and τ_C is the integration constant. To determine this constant, we assume that $\tau(\xi = 1) = \tau_0 \equiv z_0/c_{\rm k0}$, which gives $\tau_C = -\tau_0$.

We express the turning-point frequencies given by Equations (37) and (38) in terms of ξ. This gives

$$\Omega^2_{{\rm tp},v}(\xi) = \Omega^2_{\rm k0}\left[1 + 4\frac{H_{00}}{z_0} + \left(\frac{H_{00}}{z_0}\right)^2 (3 + g_1(\xi))\right]\xi^{-1} \ , \tag{42}$$

where $\Omega_{\rm k0} = c_{\rm k0}/4H_{00}$, with H_{00} being the scale height at z_0, and

$$g_1(\xi) = \frac{4\xi}{(2\xi^{1/2} - 1)^2} \tag{43}$$

and

$$\Omega^2_{{\rm tp},b}(\xi) = \Omega^2_{\rm k0}\left[1 - \left(\frac{H_{00}}{z_0}\right)^2 (1 - g_1(\xi))\right]\xi^{-1} \ . \tag{44}$$

The difference between the turning-point frequencies is

$$\frac{\Omega^2_{{\rm tp},v}(\xi) - \Omega^2_{{\rm tp},b}(\xi)}{\Omega^2_{\rm k0}} = 4\left(\frac{H_{00}}{z_0}\right)\left(\frac{H_{00}}{z_0} + 1\right)\xi^{-1} \ , \tag{45}$$

which shows that $\Omega^2_{{\rm tp},v}(\xi)$ is larger than $\Omega^2_{{\rm tp},b}(\xi)$. Hence, $\Omega_{{\rm tp},v}$ becomes the local cutoff frequency, so we write $\Omega_{\rm cut}(\xi) = \Omega_{{\rm tp},v}(\xi)$ and

$$\Omega_{\rm cut}(\xi) = \Omega_{\rm k0}\left[1 + 4\frac{H_{00}}{z_0} + \left(\frac{H_{00}}{z_0}\right)^2 (3 + g_1(\xi))\right]^{1/2} \xi^{-1/2} \ . \tag{46}$$

The local cutoff frequency $\Omega_{\rm cut}$ is plotted as a function of ξ in Figure 2. It is seen that the cutoff frequency decreases with the atmospheric height in the model with $m = 1$.

5.2. *Case of m = 2*

In this case, $\tau(\xi)$ is given by

$$\tau(\xi) = \frac{z_0}{c_{\rm k0}} ln\xi + \tau_C \ , \tag{47}$$

where τ_C is the integration constant determined from the assumption that $\tau(\xi = 1) = \tau_0 \equiv z_0/c_{\rm k0}$. This gives $\tau_C = \tau_0$. The turning-point frequencies are

$$\Omega^2_{{\rm tp},v}(\xi) = \Omega^2_{\rm k0}\left[\xi^{-2} + 8\frac{H_{00}}{z_0}\xi^{-1} + 4\left(\frac{H_{00}}{z_0}\right)^2 (1 + g_2(\xi))\right] \tag{48}$$

and

$$\Omega^2_{{\rm tp},b}(\xi) = \Omega^2_{\rm k0}\left[\xi^{-2} + 4\left(\frac{H_{00}}{z_0}\right)^2 (1 + g_2(\xi))\right] \ , \tag{49}$$

where

$$g_2(\xi) = \frac{1}{(1 + ln\xi)^2} \ . \tag{50}$$

Here $\Omega_{{\rm tp},v}(\xi)$ is always larger than $\Omega_{{\rm tp},b}(\xi)$. Thus, we choose $\Omega_{{\rm tp},v}$ as the local cutoff frequency and write $\Omega_{\rm cut}(\xi) = \Omega_{{\rm tp},v}(\xi)$, or

$$\Omega_{\rm cut}(\xi) = \Omega_{\rm k0}\left[\xi^{-2} + 8\frac{H_{00}}{z_0}\xi^{-1} + 4\left(\frac{H_{00}}{z_0}\right)^2 (1 + g_2(\xi))\right]^{1/2} \ . \tag{51}$$

This cutoff frequency is plotted as a function of ξ in Figure 2, which shows that the cutoff remains almost constant in the model with $m = 2$.

5.3. *Cases with m > 2*

In this general case of $m > 2$, we obtain

$$\tau(\xi) = \frac{z_0}{c_{\rm k0}}\left(\frac{2}{2 - m}\right)\xi^{1 - m/2} + \tau_C \ , \tag{52}$$

where the integration constant τ_C is evaluated by taking $\tau(\xi = 1) = \tau_0 \equiv z_0/c_{\rm k0}$; note that our choice of τ_0 gives the same physical parameters at $z = z_0$ for all the power-law models. After evaluating τ_C, we calculate

$$\begin{aligned}\Omega^2_{{\rm tp},v}(\xi) = \Omega^2_{\rm k0}\Bigg[&\xi^{-m} + 4m\left(\frac{H_{00}}{z_0}\right)\xi^{-1} \\ &+ m(4 - m)\left(\frac{H_{00}}{z_0}\right)^2 \xi^{m-2} \\ &+ 4\left(\frac{m - 2}{m}\right)^2\left(\frac{H_{00}}{z_0}\right)^2 g_3(\xi)\Bigg] \ ,\end{aligned} \tag{53}$$

where

$$g_3(\xi) = \left(1 + \frac{2}{m}\xi^{1 - m/2}\right)^{-2} \ , \tag{54}$$

and

$$\begin{aligned}\Omega^2_{{\rm tp},b}(\xi) = \Omega^2_{\rm k0}\Bigg[&\xi^{-m} + m(3m - 4)\left(\frac{H_{00}}{z_0}\right)^2 \xi^{m-2} \\ &+ 4\left(\frac{m - 2}{m}\right)^2\left(\frac{H_{00}}{z_0}\right)^2 g_3(\xi)\Bigg] \ .\end{aligned} \tag{55}$$

We now calculate the difference between these turning-point frequencies and obtain

$$\frac{\Omega_{\mathrm{tp},b}^2(\xi)-\Omega_{\mathrm{tp},v}^2(\xi)}{\Omega_{\mathrm{k}0}^2} = 4m(m-2)\left(\frac{H_{00}}{z_0}\right)^2 \xi^{m-2} - 4m\frac{H_{00}}{z_0}\xi^{-1} \,. \tag{56}$$

Since in this model $H_{00} > z_0$, $m > 2$, and $\xi > 1$, $\Omega_{\mathrm{tp},b}^2$ is larger than $\Omega_{\mathrm{tp},v}^2$. This indicates that the local cutoff frequency is $\Omega_{\mathrm{cut}}(\xi) = \Omega_{\mathrm{tp},b}(\xi)$, or

$$\Omega_{\mathrm{cut}}(\xi) = \Omega_{\mathrm{k}0}\left[\xi^{-m} + m(3m-4)\left(\frac{H_{00}}{z_0}\right)^2 \xi^{m-2} + 4\left(\frac{m-2}{m}\right)^2\left(\frac{H_{00}}{z_0}\right)^2 g_3(\xi)\right]^{1/2} . \tag{57}$$

The cutoff frequency calculated for the power-law temperature models with m = 3, 4 and 5 is plotted versus the distance ratio in Figure 2. It is seen that this cutoff frequency always increases with the atmospheric height in the models with $m > 2$ and that its increase is much faster for higher values of m.

5.4. *Discussion*

The effects of different temperature gradients on the cutoff frequency for transverse tube waves are presented in Figure 2. Since the cutoff frequency is a local quantity, its value at a given atmospheric height determines the frequency that the waves must exceed in order to be propagating waves at this height. Our results demonstrate that the conditions for wave propagation strongly depend on the temperature profiles.

If the temperature increases linearly with height (m = 1), the cutoff frequency starts with its maximum at $z = z_0$ and then decreases with height. For the temperature model with m = 2, the cutoff frequency remains practically constant with height. However, the cutoff frequency always increases with height in the temperature models with $m \geq 3$; the higher the value of m, the steeper an increase of the local cutoff frequency with height is observed.

The main purpose of using the power-law temperature models was to demonstrate the dependence of the local cutoff frequency on the increasing steepness of the temperature models. Obviously, the power-law models do not properly describe the temperature gradients in the solar atmosphere. Therefore, we now consider a more realistic model of the solar atmosphere.

6. VAL MODEL OF THE SOLAR ATMOSPHERE

We assume that a thin flux tube is embedded in the reference mean solar atmosphere model VAL-C (Vernazza et al. 1981). In this model, the height z = 0 km corresponds to unity optical depth, where the temperature is 6420 K. Beyond the temperature minimum T_{min} = 4170 K, which is located at z = 515 km, the model extends through the chromosphere well into the transition region to the corona, up to a temperature of 4.47×10^5 K. At the base of the transition region the VAL-C model exhibits a plateau with a temperature around 2×10^4 K, caused by Lyα emission. This plateau was later shown to disappear if the physics of the transition region is treated more realistically (Fontenla et al. 1990). Therefore we restrict ourselves to the height range from $z = z_0$ = 0 km (optical depth unity) to the just below the plateau (z = 2 113 km).

To calculate the characteristic wave speed c_{k} as a function of z, we have to know the magnetic field $B_0(z)$, which is not given in the VAL-C model. Since the tube is assumed to be in in thermal equilibrium with its surroundings at each atmospheric height, we use the local value of the pressure scale height, which is the same outside and inside the tube, to evaluate $B_0(z)$; the calculation begins with an assumed surface magnetic field $B_0(z_0)$ = 1500 G (see Equation (1)). Having obtained the distribution of the tube magnetic field with height, we then calculate the gas pressure and density inside the tube, and the characteristic wave speed $c_{\mathrm{k}}(z)$ (see Equation (3)). In the lower panel of Figure 3 we plot c_{k} versus the atmospheric height in the model; for comparison we also plot the sound speed c_{S}. The results show that c_{k} is smaller than c_{S} in almost the entire model, except in the upper chromosphere and lower transition region, where c_{k} becomes comparable to, or even slightly larger than, c_{S}.

In order to calculate the wave propagation time τ, we use Equation (29). For the integration constant $\tau_C = \tau(z = 0) = \tau_0$ we choose a value of 100 s, thus assuming that the waves have traveled for 100 s before they reach the base z_0 of the model. For typical wave speeds (cf. lower panel of Figure 3) this means that the waves are generated about two scale heights below z_0.

To determine the cutoff frequency $\Omega_{\mathrm{cut}}(z)$ according to Section 4.5, we calculate both turning-point frequencies $\Omega_{\mathrm{tp},v}(z)$ and $\Omega_{\mathrm{tp},b}(z)$ and select the larger one as $\Omega_{\mathrm{cut}}(z)$ (see Equations (33), (34), and (37)–(39)). To perform these calculations, we must evaluate the first derivative of c_{k} and H, and the second derivative of c_{k}. These calculations have to be done numerically because the model consists of tabulated data. The upper panel of Figure 3 shows the resulting cutoff frequency $\Omega_{\mathrm{cut}}(z)$ as well as Spruit's cutoff frequency $\Omega_{\mathrm{k}}(z) = c_{\mathrm{k}}(z)/4H(z)$ (cf. Equation (12)), where the latter is again treated here as a local, height-dependent quantity.

A striking property of Figure 3 is that the cutoff frequency for the nonisothermal case, $\Omega_{\mathrm{cut}}(z)$, is wiggly. This is mostly caused by the dependence of the turning-point frequencies on the second derivative of the tube speed c_{k} (cf. Equations (33) –(34)). Since the VAL-C model is specified by a number of tabulated distinct points, the curves in Figure 3 must be plotted by finding interpolating or fitting functions through these points and determining the first derivative of the scale height, and the first and second derivatives of the tube speed, in order to calculate the terms in Equations (33)–(34). Such derivatives of interpolated curves tend to show a wiggly behavior. As shown in the middle and lower panels of Figure 3, these wiggles are stronger near the temperature minimum and in particular at the foot of the transition region, where the gradients change rapidly (see also Fawzy & Musielak 2012).

One could avoid the wiggles by approximating the data by simple functions with known smooth derivatives. There are also automatic algorithms that can smooth out such wiggles more or less completely (e.g., Chartrand 2011). However, we show them here explicitly in order to illustrate the dependence of the cutoff frequency, via these derivatives, on the nature of the solar atmosphere, which in reality is less homogeneous than the VAL-C model and in addition temporally variable. Therefore, we chose the well-proven algorithm by Reinsch (1967), which fits the data points by a natural cubic spline, thus giving consistent first and second derivatives. A moderate amount of smoothing can be applied, so that the spline needs not go exactly through the points.

Since the value of Ω_{cut} is different at each atmospheric

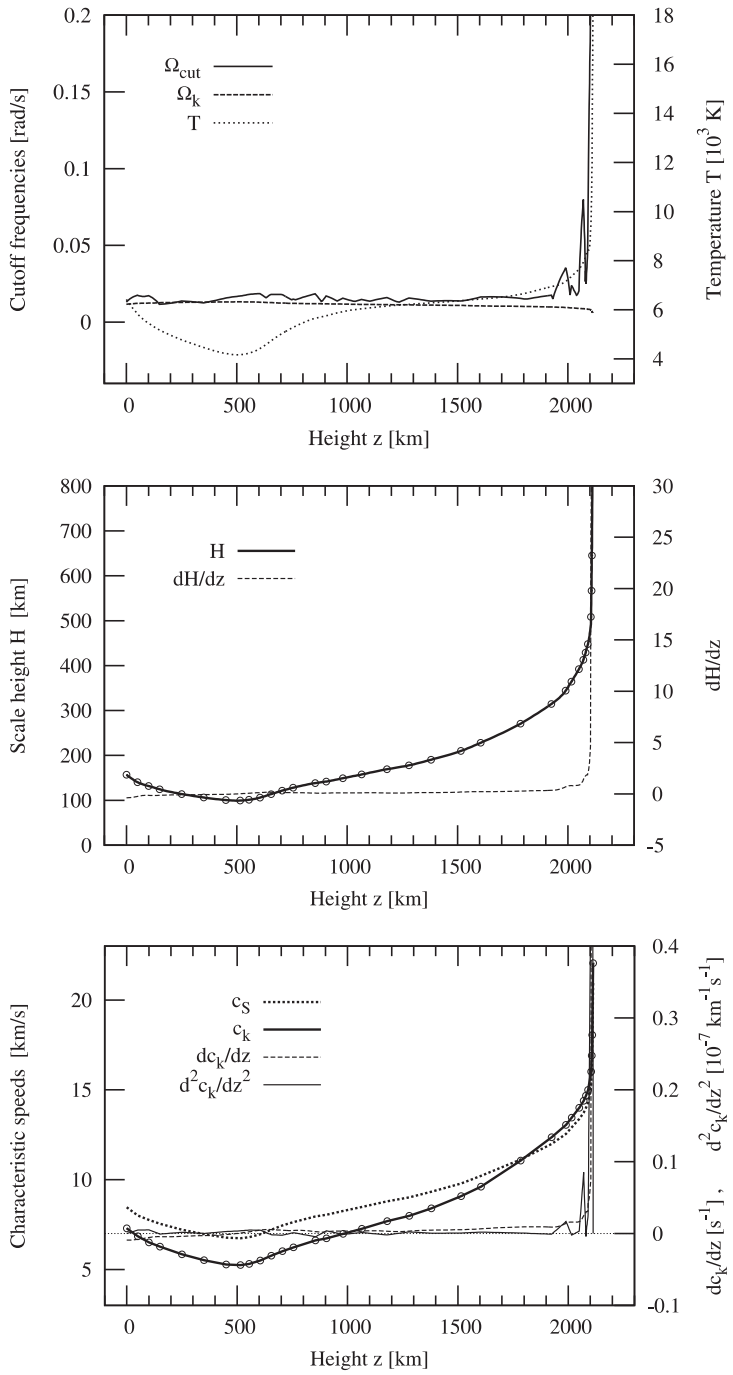

Figure 3. The *upper panel* shows the height dependence of the cutoff frequency $\Omega_{\rm cut}$ for the VAL-C model, for which the temperature stratification is shown as a dotted line scaled with the right y axis. For comparison, Spruit's isothermal cutoff frequency $\Omega_{\rm k} = c_{\rm k}/4H$ is plotted by using local values of the tube speed $c_{\rm k}$ and the scale height H. The *middle* and *lower* panels, respectively, show H and $c_{\rm k}$ as well as the sound speed $c_{\rm S}$, with scales on the left y axes. The values of H and $c_{\rm k}$ at the tabulated points of the VAL-C model are marked with circles. The derivatives of the spline curves through these points are shown with scales on the right y axes.

height, the frequency ω of a transverse tube wave must be higher than the cutoff at a given height z in order to be propagating at this height. Overall, the new cutoff frequency $\Omega_{\rm cut}$ is seen to be slightly higher than $\Omega_{\rm k}$ throughout the chromosphere. This is mostly caused by the fact that the chromospheric temperature increases with height, leading to a positive first derivative of the tube speed $c_{\rm k}$, which increases both turning-point frequencies (cf. Equations (33) and (34)) and thus also their maximum, the cutoff frequency $\Omega_{\rm cut}$ (Equation (39)).

Another difference between the Spruit cutoff and our new result lies in the behavior at the foot of the transition region. Here $\Omega_{\rm k}$ decreases with height (which becomes more evident if one continues the calculation to higher levels of the VAL-C model), while $\Omega_{\rm cut}$ increases rapidly as we approach the steep temperature rise in the transition region. Formally this means that a wave with arbitrary frequency tends to lie above $\Omega_{\rm k}$ at the transition region (implying propagation in the case of an isothermal treatment of the cutoff), but below our value (implying reflection off the temperature gradient in our non-

isothermal treatment). This may have implications for the contribution of such transverse waves to the heating and dynamics of the overlying corona. However, we put not much weight on such differences in the high chromosphere and transition region, fow two reasons. First, we have not provided a complete study of the reflection properties of the transition region, which would require a more complex analysis of the complete solar atmosphere. And second, a basic approximation underlying all these theories breaks down much earlier, already in the mid chromosphere - namely, that the flux tubes can be approximated as thin. The thin flux tube approximation, which is the basis for the results presented in this paper and for Spruit's results as well, is no longer valid at those heights. Thus the results obtained for the upper atmosphere must be taken with caution. We have extended the calculations up to the foot of the transition region in order to determine the approximate behavior of the cutoffs in these layers, even though this is beyond the formal limit of validity of our analytical results, because the presented results demonstrate that the temperature gradient in the upper solar chromosphere and in the solar transition region will have a major influence on the propagation of transverse tube waves.

The increase of temperature with height requires atmospheric heating, which is typically identified with acoustic-gravity and flux tube waves, including transverse tube waves, or with phenomena related to magnetic reconnection (e.g., Priest 1982; Narain & Ulmschneider 1996; Ulmschneider & Musielak 2003). Our results presented in Figure 3 give constraints on the range of frequencies of transverse tube waves that are propagating in different parts of the solar atmosphere.

Our results show that in the upper photosphere and lower chromosphere $\Omega_{\rm cut}^{\rm phot} \approx 0.01\,{\rm rad/s}$, or the cutoff period is 500 s, and that in the middle and upper chromosphere $\Omega_{\rm cut}^{\rm chrom} \approx 0.02\,{\rm rad/s}$, which corresponds to the cutoff period of 350 s. As already mentioned in Section 1, Fujimura & Tsuneta (2009) observed transverse tube waves with periods of 240-540 s, or the corresponding frequency range $\omega \approx (0.01 - 0.03)\,{\rm rad/s}$, in intergranular magnetic elements. Comparison of these observational results to our theoretical cutoff frequencies shows that most of the observed waves are freely propagating in the solar photosphere and lower chromosphere because $\omega > \Omega_{\rm cut}^{\rm phot}$, however, in the middle and upper parts of the solar chromosphere the waves with frequencies $\omega < \Omega_{\rm cut}^{\rm chrom}$ are not propagating.

Now, the high frequency waves with periods of 45 s, or $\omega \approx 0.1\,{\rm rad/s}$, observed by Okamoto & De Pontieu (2011) along spicules do satisfy the condition $\omega > \Omega_{\rm cut}^{\rm chrom}$ and they are obviously freely propagating waves in the solar chromosphere. Similarly, the high frequency oscillations with periods ranging from 30 s to 180 s, which corresponds to the frequency range $\omega \approx (0.03 - 0.2)\,{\rm rad/s}$, detected by Yurchyshyn et al. (2012) in type II spicules also satisfy the condition $\omega > \Omega_{\rm cut}^{\rm chrom}$, and therefore they are freely propagating waves in the solar chromosphere.

The above constraints can be used to assess the role of transverse tube waves in the heating and dynamics of the solar atmosphere. As discussed by Hasan & Kalkofen (1999), Musielak & Ulmschneider (2003), and Hasan (2003), transverse tube waves may be responsible for the excitation of solar atmospheric oscillations observed in magnetically active regions near sunspots. The results obtained in this paper can be used to determine the natural frequency of the solar atmosphere inside thin and non-isothermal magnetic flux tubes and the effects of temperature gradients on solar atmospheric oscillations.

7. CONCLUSIONS

Our method to determine the cutoff frequency for transverse waves propagating along a thin and non-isothermal flux tube requires that integral transformations are used to cast the wave equations for both wave variables in the standard forms. Then the conditions for the existence of propagating wave solutions are established by using the oscillation theorem. The theorem is also used to obtain the turning-point frequency for each wave variable. The larger among the two turning-point frequencies is selected as the cutoff frequency.

To study the effects of temperature gradients on the cutoff frequency, we used different power-law temperature distributions. For the temperature that increases linearly with height, the cutoff frequency is large at the bottom of the model and then decreases with height. For the temperature profile with the power of 2, the cutoff frequency remains practically constant with height. However, for powers higher than 2, the cutoff frequency always increases with height; and the higher the power, the steeper the increase of the cutoff frequency with height.

We also calculated the cutoff frequency $\Omega_{\rm cut}$ as a function of height z in the VAL-C model and compared it to Spruit's global cutoff frequency Ω_S that was treated as a height-dependent quantity. The comparison shows that $\Omega_{\rm cut}$ exceeds Ω_S, and that the differences are especially prominent in the upper parts of the model, where however the thin flux tube approximation is not valid any longer. The differences in the lower atmosphere, where the thin flux tube approximation is valid, may be important for the energy carried by transverse tube waves from the solar convection zone, where the waves are generated, to the overlying solar atmosphere, where the wave energy is deposited.

The cutoff frequency $\Omega_{\rm cut}$ calculated for the VAL-C model gives constraints on the range of frequencies of transverse tube waves that are propagating in different parts of the solar atmosphere. We compared $\Omega_{\rm cut}$ to the range of frequencies determined from observations by Fujimura & Tsuneta (2009), Okamoto & De Pontieu (2011), and Yurchyshyn et al. (2012). Based on this comparison, we established that most of the waves observed by Fujimura & Tsuneta (2009) in intergranular magnetic elements are freely propagating in the solar photosphere and lower chromosphere, however, in the middle and upper solar chromosphere the lower frequency part of these waves corresponds to non-propagating waves. On the other hand, all the waves detected by Okamoto & De Pontieu (2011) and Yurchyshyn et al. (2012) in spicules are freely propagating waves in the solar chromosphere.

These constraints are important for understanding the role played by transverse tube waves in the heating of the solar atmosphere and in the acceleration of plasma, e.g. in spicules and the solar wind. Our results can be used to determine the natural frequency of the solar atmosphere inside thin and non-isothermal flux tubes and to study the effects of the temperature stratification on the excitation of atmospheric oscillations inside solar magnetic flux tubes.

Z.E.M. acknowledges the support of this work by the Alexander von Humboldt Foundation.

REFERENCES

Aghajani, A., & Roomi, V. 2012, Turk. J. Math. 36, 273
Antolin P., Shibata K., Kudoh T., Shiota D., & Brooks D. 2009, in ASP Conf. Ser. 415, The Second Hinode Science Meeting: Beyond Discovery-Toward Understanding, ed. B. Lites, M. Cheung, T. Magara, J. Mariska, & K. Reeves (San Francisco: ASP), 247
Bogdan, T. J., Hindman, B. W., Cally, P. S., & Charbonneau, P. 1996, ApJ, 465, 406B
Bohner, M., & Ünal, M. 2005, J. Phys. A: Math. Gen., 38, 6729
Bonet, J. A., Marquez, I., Sanchez Almeida, J., Cabello, I., & Domingo, V. 2008, ApJ 687, 431
Bonet, J. A., et al. 2010, ApJ, 723, L139
Chartrand, R. 2011, ISRN Appl Math, Vol. 2011, 164564
Cirtain, J. W., et al. 2007, Science, 318, 1580
Defouw, R. J. 1976, ApJ, 209, 226
De Pontieu, B., et al. 2007, Science, 318, 1574
De Pontieu, B., et al. 2012, ApJ, 752, L12
Fawzy, D. & Musielak, Z. E., 2012, MNRAS, 412, 159
Ferriz-Mas, A., Schüssler, M., & Anton, V. 1989, A&A, 210, 425
Fite, W. B. 1918, Trans. Amer. Math. Soc., 19, 341
Fontenla, J. M., Avrett, E. H. & Loeser, R., 1990, ApJ, 355, 700
Fujimura, D., & Tsuneta, S. 2009, ApJ, 702, 1443
Hammer, R., Musielak, Z. E., & Routh, S. 2010, AN, 331, 593
Hasan, S. S., 2003, in Lectures on Solar Physics, ed. H. M. Antia, A. Bhatnagar, & P. Ulmschneider (Lecture Notes in Physics, Vol. 619; Berlin: Springer), 173
Hasan, S. S., 2008, AdSpR, 42, 86
Hasan, S. S., & Kalkofen, W. 1999, ApJ, 519, 899
Hille, E. 1948, Trans. Amer. Math. Soc., 64, 234
Hollweg J. V. 1985, in: Advances in Space Plasma Physics, B. Buti, Ed., World Scientific Publ., Singapore, p. 77
Jess, D. B., Mathioudakis, M., Erdelyi, R., Crokett, P. J., Keenan, F. P., & Christian, D. J. 2009, Science 323, 1582
Kahn, P. B. 1990, Mathematical Methods for Scientists and Engineers, John Wiley, New York
Kneser, A. 1893, Math. Ann., 42, 409
Lamb, H. 1908, Proc. Lond. Math. Soc. 2, 122
Lamb, H. 1975, Hydrodynamics, Cambridge Uni. Press, Cambridge
Lee, C.-F., Yeh, C.-C., & Gau, C.-Y. 2005, Czechoslovak Math. J., 55, 845
Leighton, W. 1950, Duke Math. J. 17, 57
Leighton, W. 1962, Proc. Amer. Math. Soc. 13, 603
Li, W. 1998, J. Math. Anal. Appl. 217, 1
Li, H. J., & Yeh, C.C. 1995, Proc. Roy. Soc. Edin., 125A, 1193
Li, H. J., & Yeh, C.C. 1996, Math. Nachr., 182, 295
McIntosh, S. W., et al. 2011, Nature 475, 477
Murphy, G. M. 1960, Ordinary Differential Equations and Their Solutions, D. Van Nostrand Company, New York
Musielak, Z. E., Fontenla, J. M., & Moore, R. L. 1992, Phys. Fluids, 4, 13
Musielak, Z. E., & Moore, R. L. 1995, ApJ, 452, 434
Musielak, Z. E., Musielak, D. E., & Mobashi, H. 2006, Phys. Rev. E, 73, 036612-1
Musielak, Z. E., Rosner, R., Gail, H. P., & Ulmschneider, P. 1995, ApJ, 448, 865
Musielak, Z. E., Rosner, R., & Ulmschneider, P. 1987, in Lecture Notes in Physics 291: Cool Stars, Stellar Systems and the Sun, eds. J. L. Linsky & R. E. Stencel, Berlin: Springer, 66
Musielak, Z. E., Routh, S., & Hammer, R. 2007, ApJ, 659, 650
Musielak, Z. E., & Ulmschneider, P. 2001, A&A, 370, 541
Musielak, Z. E., & Ulmschneider, P. 2003, A&A, 406, 725
Narain, U., Ulmschneider, P. 1996, Space Sci. Rev., 75, 453
Okamoto, T. J., & De Pontieu, B., 2011, ApJ, 736, L24
Petukhov, M. Yu. 2006, Astron. Lett. 32, 418
Priest, E. R. 1982, Solar Magnetohydrodynamics, Dordrecht-Reidel
Rae, I. C., & Roberts, B. 1982, ApJ, 256, 761
Reinsch, C. R. 1967, Num. Math., 10, 177
Roberts, B. 1979, Sol. Phys., 61, 23
Roberts, B. 1981, in Physics of Sunspots, L. E. Cram & J. H. Thomas, Eds., Sacramento Peak, New Mexico, 360
Roberts, B. 1991, Geophys. Astrophys. Fluid Dynamics, 62, 83
Roberts, B., & Ulmschneider, P. 1997, in: Solar and Heliospheric Plasma Physics, Simett G. M., Alissandrakis C. E., Vlahos L., Eds., Springer-Verlag, Berlin, p. 75
Roberts, B., & Webb, A.R. 1978, Sol. Phys. 56, 5
Routh, S., Musielak, Z. E., & Hammer, R. 2007, Sol. Phys. 246, 133
Routh, S., Musielak, Z. E., & Hammer, R. 2010, ApJ, 709, 1297
Schmitz, F., & Fleck, B. 1998, A&A 337, 487
Schmitz, F., & Fleck, B. 2003, A&A 399, 723
Solanki, S. K. 1993, Space Sci. Rev., 63, 1
Spruit, H. C. 1981, A&A 98, 155
Spruit, H. C. 1982, Sol. Phys. 75, 3
Stix, M. 1991, The Sun - An Introduction, 2nd ed. (Berlin: Springer)
Sturm, C. 1836, J. Math. Pures Appl., 1, 106
Swanson, C. A. 1968, Comparison and Oscillation Theory of Linear Differential Equations, Academic Press, New York and London
Teschl, G. 2011, Ordinary Differential Equations and Dynamical Systems, (Providence, RI: AMS)
Tomczyk, S., et al. 2007, Science, 317, 1192
Tyagi, J. 2009, Electronic J. Diff. Eqs 19, 1
Ulmschneider, P., & Musielak, Z.E. 2003, in 21st NSO/SP Workshop on Current Theoretical Models and Future High Resolution Solar Observations: Preparation for ATST, A.A. Pevtsov and H. Uitenbrock (Eds), ASP Conf. Ser., 286, 363
Van Doorsselaere T., Nakariakov V. M., Verwichte E., 2008, ApJ, 676, L73
Vernazza, J. E., Avrett, E. H., & Loeser, R., 1981, ApJS, 45, 635
Wedemeyer-Böhm, S., & Rouppe van der Voort, L., 2009, A&A, 507, L9
Wedemeyer-Böhm, S., et al. 2012, Nature 486, 505
Wintner, A. 1949, Quat. Appl. Math., 7, 115
Wintner, A. 1957, Math. Scand. 5, 255
Wong, J. S. W. 1996, Meth. Appl. Analysis 3, 476
Yurchyshyn, V., Kilcik, A., & Abramenko, V. 2012, arXiv:1207.6417v1